Hindawi
Advances in Astronomy
Volume 2023, Article ID 4548171, 17 pages
https://doi.org/10.1155/2023/4548171

Research Article

Propagation of Nonlinear Dust-Acoustic Waves in a Self-Gravitating Collision Magnetized Dusty Plasma in Earth's Magnetosphere

Aljawhara H. Almuqrin,[1] Mohammed F. Alotiby,[2] and R. E. Tolba[3]

[1] *Department of Physics, College of Science, Princess Nourah Bint Abdulrahman University, P.O. Box 84428, Riyadh 11671, Saudi Arabia*
[2] *Nuclear Technologies Institute (NTi), King Abdulaziz City for Science & Technology (KACST), P. O. Box 6086, Riyadh 11442, Saudi Arabia*
[3] *Centre for Theoretical Physics, The British University in Egypt (BUE), El-Shorouk City, Cairo, Egypt*

Correspondence should be addressed to R. E. Tolba; reda.tolba@bue.edu.eg

Received 3 March 2023; Revised 20 May 2023; Accepted 6 June 2023; Published 29 June 2023

Academic Editor: Xiao Ping Zhang

The nonlinear propagation of different types of DANW acoustic dust nonlinear waves has been investigated in a magnetized dusty plasma consisting of negatively charged dust particles, Maxwellian electrons, and ions. Application of the standard reductive perturbation theory is used to derive the corresponding three-dimensional nonlinear a complex Ginzburg–Landau (3D-CGLE) equation which governs the dynamics of the dust-acoustic wave packets. The stationary analytical solutions of the CGLE are numerically analysed where the effect of the physical parameters of the dusty plasma model on the wave's propagation is taken into account. It has been found that there can be a relationship between the appearance of soliton waves and electromagnetic waves, as well as between shock-like waves and periodic travelling waves. Expression of the importance of these findings is the cornerstone of explaining the true relationship between the propagation of nonlinear waves in the physics of space, for example, the Earth's magnetic field.

1. Introduction

Wave propagation and instability in magnetic dusty plasmas have been studied extensively in the past few decades since the presence of charged dust particles is so massive that it plays a definitive role in understanding and interpreting electrostatic disturbances in space plasma environments as well as in laboratory plasmas. One of the main properties of gases in plasma conditions is the transfer of radiant energy. This is because it is considered to be an obvious consequence of the excitation of high-energy states of elementary particles in the plasma and the way they revert to lower or lower-energy states, or it can be the ground state, by emitting radiation over a wide range of the spectrum. Thus, we find that the presence of the magnetic field in the various astrophysical plasma environments has a very effective role in modifying the properties and behavior of nonlinear wave propagation in these media [1, 2]. Among the exciting studies conducted in the presence of the magnetic field in plasma environments, it was observed that when gravitational waves propagate in the various cosmic environments, they interact with a small magnetic field, and thus, they produce electromagnetic radiation [3, 4]. With many different types of plasma medium, we found that the magnetic field exerts a force known as the Lorentz force that affects the moving charged particles, which penetrates or diverts the transport path of the charged particles into a spiral, and this, in turn, affects the properties and the formation of nonlinear structures in this manner [5–7]. Recently, it has also been established for the theoretical study, and for dusty plasma physics, there is an unstable spectrum of genes in nonmagnetic and self-gravitational dust gases. Therefore, it has been shown that in dusty nonmagnetic gases, instability of densities occurs from the presence of ion dust-acoustic waves or dust-acoustic waves [8–10]. Thus, it happens that very large dust grains are exposed to other types of forces that affect them, for example, both electrostatic forces as well as gravitational forces while the effect on both ions and electrons is sometimes tested by electrical force only because their masses are much smaller compared to the mass of dust. Thus, we find that the instability expressed by jeans has a very important and effective role in the phenomenon of the collapse of dusty grains as well as dusty molecular clouds [11].

Since most astrophysical phenomena contain strong magnetic fields and inhomogeneous equilibrium densities, it is important to consider the study of electrostatic waves of self-gravitational ferromagnetic gases that can be classified as homogeneous or heterogeneous. In the stable Pinnjjmal clouds, we find a dusty plasma probe study that can be described in self-gravitational magnetic fields [12–14].

The propagation phenomenon and properties of ion-acoustic waves were studied in a nonmagnetic electron-ion plasma, which is characterized by a non-Maxwellian confined electron distribution, in addition to a kappa distribution function with a Schamel distribution. Where the reductionist perturbation theory was applied to obtain the nonlinear and nonplanar Schamel Burgers equation using the basic field equation. Where they found that the effect of viscosity, may cause collisions that lead to the emergence of anomalous dissipation, which usually results in a wave solution of the shock waves. It was found from the investigation in this study that the effects of both viscosity and collisions may cause thumping dissipation [15]. In a dusty, nonmagnetic collisional plasma containing negatively charged dust grains, positive ions, neutral particles, and Maxwellian electrons. The solution was obtained, and shocks were found for the propagation of dust ionic sound waves. Furthermore, assuming that a conservation law is applied in the system, they obtain an approximate solution for the solitary wave, although the existence of the Burgers term causes an increase in the viscosity effect and thus opposes the a conservation law in the system. Thus, in this case, the shock may be a generated wave that occurs due to the strong effect of anomalous dissipation. Knowing the proof, Hirota's simplified bilinear method was used, and the waveform solution known as shock type was obtained. Again, when the dissipation was weak, the balance between dispersion and nonlinearity could result in a singular solution. Taking into consideration, the case of weak dissipation, the single-wave solution was explored directly without taking into account the conservation law by applying a residual weighted method [16]. The nonlinear analysis of the solitary ion acoustic solutions as well as the shock wave solutions of the nonwide earth plasma has been investigated under the modified Korteweg-de Vries-Burgers equation. The nonlinear analysis of the single ion acoustic solutions as well as the nonwide ground plasma shock wave solutions was investigated under the modified Korteweg-de Vries-Burgers equation where the different patterned solutions of the MKdV equation were derived directly from the corresponding Hamiltonian of the system, using the weighted residual method. Thus, approximate analytical solutions of the MKdVB equation are explored using the solution of the MKdV equation as an initial solution [17]. The propagation of EA waves in viscous plasmas is described and monitored taking into account the weak damping (by adding a Burger term) due to interparticle collisions and viscosity. Particular attention was paid to studying the effect of the physical factors present in the plasma system on wave propagation in the framework of Schamel Burgers medium [18]. The propagation properties of dust, ions, and acoustic waves in nonmagnetic dusty plasma, which consist of mobile ions, negatively charged dust particles, and also trapped non-Maxwellian electrons, as well as both the kappa distribution function and the Schamel distribution, were investigated and studied together. The effect of collisions between particles is neglected during studies of wave dynamics in a dusty plasma environment although these effects may have a significant impact on wave formation. For the first time, a large collision effect was developed in the nonplanar Schamel framework, and by using the conservation law, the approximate analytical solution of the NDS equation was derived. Also, the important effect of the damping coefficient has been described from the point of view of numerical analysis. This is in addition to examining the effects of other physical parameters on the propagation of dust waves in NDS media [19].

Recently, there has been a great interest in studying ways to obtain solutions to nonlinear differential equations (PDEs) that describe the various physical plasma phenomena. For examples of these methods are, the inverse scattering method and a generalized exponential method of solution of several physically interesting, nonlinear partial differential equations (PDEs), such as the nonlinear Schröinger equation (NLSE), Korteweg-de Vries equation (KdV), Kadomtsev-Petviashvili equation, and Sine-Gordon equation [20–24]. These methods, in fact, are able to express the solutions of integrable differential equations and obtain various waves when one of these analytical methods is used to obtain the solution. The physical phenomena in which the above fully integrable nonlinear differential equations (PDEs) arise tend to be very idealistic in dealing with those equations. Therefore, including influences such as damping, external forces, and an inhomogeneous medium in a dusty plasma (e.g., a medium with variable density or depth) may provide a more realistic model to explain those phenomena whereas the inclusion of these perturbation effects would imply that the PDE is no longer fully integrable, and hence, it is important to define the conditions under which the perturbed PDE is fully integrable in order to be able to describe and study different physical phenomena [25, 26].

The complex Ginzburg–Landau (CGLE) equation is a nonlinear differential equation rich in a number of solutions that contain critical values, so it has an effective and essential role in understanding nonlinear wave physics in many nonequilibrium phenomena, especially in dusty plasma physics. A review of specific physical systems which are described by this equation can be found in [27, 28]. However, the physical states are described by the two- and three-dimensional CGLE emerge frequently. It is therefore of attention to study the characteristics solutions of the multidimensional CGLE. In other words, CGLE is the amplitude equation suitable for describing the slow dynamics in the supercritical transition to unidirectional travelling waves [29–31].

Motivated by these theoretical works are the following:

(1) Investigate the stability of dust sound waves in the Earth's magnetic field condition

(2) Determine which condition gives rise to both the Soliton wave and the periodic wave when the same solution is used to obtain both waves

(3) Determine which condition gives rise to both the shock-like wave and the periodical wave, and also when the same solution is used to obtain them

(4) Describe the magnetosonic waves that may appear in Earth's magnetic field

The following is a summary of this work. In Section 2, we give the relevant dynamical equations, i.e., the equations for the negatively charged dusty plasma fluid, put it into a dimensionless form, and give the electrons and ions associated with them by the equation of neutrality. In Section 3, the standard reductive perturbation theory is used to derive the nonlinear evolution equation, which describes the system of dusty plasma. In Section 4, where two analytical solutions are presented to the evolution equation, and from these solutions, we obtain solutions for the nonlinear dust sound waves of CLGE. In Section 5, we investigate the effects of the plasma parameters in the model, and the role they play in influencing the behavior of the dust-acoustic waves. Finally, Section 6, we obtained a summary of the conclusions about the nonlinear waves describing the dusty plasma system.

2. Basic Equations and Formulation

We consider three-dimensional nonlinear, self-gravitational, magnetization, and collision nonlinear electrostatic wave propagation consisting of three components, namely, dust grain beam, electrons, and ions following the Boltzmann distribution. The magnetic field effect is considered in the z-direction only. The nonlinear dynamic process of such kind of disturbances is governed by the dust grain beam fluid equations [32, 33]

$$\frac{\partial n_d}{\partial t} + \frac{\partial}{\partial x}\left(n_d u_{dx}\right) + \frac{\partial}{\partial y}\left(n_d u_{dy}\right) + \frac{\partial}{\partial z}\left(n_d u_{dz}\right) = 0, \tag{1}$$

$$\left\{\begin{array}{c}\left(1+\tau_r\dfrac{d}{dt}\right)\left(\dfrac{du_{dz}}{dt} + v_d u_{dz} - \left(\rho_d c\right)^{-1}(J\times B) + \rho_d^{-1}\nabla P_t - \dfrac{eZ_{d0}}{m_d}(1-R)\nabla\phi + \nabla\varphi_g\right)\\ = \rho_d^{-1}\eta_0\nabla^2 u_d + \rho_d^{-1}\left(\Psi + \dfrac{\eta_0}{3}\right)\nabla\left(\nabla . u_{dz}\right).\end{array}\right\}, \tag{2}$$

where Ψ and η_0 denote the dust shear viscosity and the bulk viscosity coefficient, respectively. We thus consider the densities of both electron and ion numbers to be the Maxwellian distribution, respectively,

$$n_e = n_{e0}\exp\left(\frac{e\varphi}{K_B T_e}\right), \tag{3}$$

$$n_i = n_{i0}\exp\left(\frac{-e\phi}{K_B T_i}\right). \tag{4}$$

The total pressure contains the pressure of the electron-ion gas and the pressure of thermal radiation together [32]

$$P_t = P_e + P_i + \frac{\alpha_r}{3}\left(T_e^4 + T_i^4\right). \tag{5}$$

The equation for magnetic induction is given by

$$\frac{\partial B}{\partial t} + \left(u_{dz}.\nabla\right)B_z - \frac{1}{\mu_z\sigma_z}\nabla^2 B_z - \left(B_z.\nabla\right)u_{d_z} = 0, \tag{6}$$

where the current density is

$$J = \frac{c}{4\pi}(\nabla\times B). \tag{7}$$

Poisson's equation of gravitational potential is given by

$$\nabla^2\varphi_g = 4\pi G n_d. \tag{8}$$

The DA wave potential φ is obtained from Poisson's equation

$$\nabla^2\varphi = 4\pi e\left(Z_{d0}n_d - n_i + n_e\right). \tag{9}$$

At the equilibrium state, we have the quasineutrality condition that can be expressed as $n_{i0} = n_{e0} + Z_{d0}n_{d0}$, where Z_{d0} denotes the average number of electrons present on a grain of dust, while n_{d0} denotes the number density of undisturbed dust and finally φ_g denotes the gravitational potential. Where the three-dimensional Cartesian coordinate system is $\nabla = (\partial/\partial x, \partial/\partial y, \partial/\partial z)$, n_{i0} and n_{e0} denote the undisturbed number densities of both ions and electrons, respectively, B is the magnetic field in the direction of wave propagation z, i.e., $(B = B_z\widehat{z})$, K_B denotes the Boltzmann constant, e denotes the magnitude of the electron charge, and T_e and (T_i) are the electron and ion temperatures where $\alpha_r = (\pi K_B^4)/(15(c\hbar)^3)$ is radiation constant [32, 34].

3. Derivation of the CGL Equation

Let us now consider the system of negative dusty plasma in three-dimensional nonlinear DAWs propagating along the z axis in a Cartesian coordinate system. The dynamics of the DAWs can be described by the nonlinear fluid equations [32]

$$\frac{\partial n_d}{\partial t}+\frac{\partial}{\partial x}\left(n_d u_{\mathrm{dx}}\right)+\frac{\partial}{\partial y}\left(n_d u_{\mathrm{dy}}\right)+\frac{\partial}{\partial z}\left(n_d u_{\mathrm{dz}}\right)=0, \tag{10}$$

and the generalized viscoelastic dust momentum equation

$$\left(1+a_1\frac{\partial}{\partial t}\right)\begin{pmatrix}\dfrac{\partial u_{\mathrm{dz}}}{\partial t}+\dfrac{5}{3}n_d^{-1/3}\left(\sigma_e\mu_e+\sigma_i\mu_i\right)\dfrac{\partial n_d}{\partial z}+\\ \dfrac{8}{9}n_d^{2/3}\left(\sigma_{er}+\sigma_{ir}\right)\dfrac{\partial n_{dz}}{\partial z}-\left(1-R_1\right)\dfrac{\partial\phi}{\partial z}+\sigma_g\dfrac{\partial\varphi_g}{\partial z}\end{pmatrix}-\left(\beta_1+\beta_2\right)\frac{\partial^2 u_{\mathrm{dz}}}{\partial z^2}=0, \tag{11}$$

$$\left(1+a_1\frac{\partial}{\partial t}\right)\begin{pmatrix}\dfrac{\partial u_{\mathrm{dx}}}{\partial t}-s_1 n_d^{-1}B_z\left(\dfrac{\partial B_z}{\partial y}\right)+\dfrac{5}{3}n_d^{-1/3}\left(\sigma_e\mu_e+\sigma_i\mu_i\right)\dfrac{\partial n_d}{\partial x}+\\ \dfrac{8}{9}n_d^{2/3}\left(\sigma_{er}+\sigma_{ir}\right)\dfrac{\partial n_d}{\partial x}-\left(1-R_1\right)\dfrac{\partial\phi}{\partial x}+\sigma_g\dfrac{\partial\varphi_g}{\partial x}\end{pmatrix}-\left(\beta_1+\beta_2\right)\frac{\partial^2 u_{\mathrm{dx}}}{\partial x^2}=0, \tag{12}$$

$$\left(1+a_1\frac{\partial}{\partial t}\right)\begin{pmatrix}\dfrac{\partial u_{\mathrm{dy}}}{\partial t}-s_1 n_d^{-1}B_z\left(-\dfrac{\partial B_z}{\partial x}\right)+\dfrac{5}{3}n_d^{-1/3}\left(\sigma_e\mu_e+\sigma_i\mu_i\right)\dfrac{\partial n_d}{\partial y}+\\ \dfrac{8}{9}n_d^{2/3}\left(\sigma_{er}+\sigma_{ir}\right)\dfrac{\partial n_d}{\partial y}-\left(1-R_1\right)\dfrac{\partial\phi}{\partial y}+\sigma_g\dfrac{\partial\varphi_g}{\partial y}\end{pmatrix}-\left(\beta_1+\beta_2\right)\frac{\partial^2 u_{\mathrm{dy}}}{\partial y^2}=0, \tag{13}$$

$$n_e=\exp\left(\sigma_e\phi\right), \tag{14}$$

$$n_i=\exp\left(-\sigma_i\phi\right), \tag{15}$$

$$P_t=P_{i0}\left(\frac{n_d}{n_{i0}}\right)^{5/3}+P_{e0}\left(\frac{n_d}{n_{e0}}\right)^{5/3}+\frac{a_r}{3}T_e^4\left(\frac{n_d}{n_{e0}}\right)^{8/3}+\frac{a_r}{3}T_i^4\left(\frac{n_d}{n_{i0}}\right)^{8/3}, \tag{16}$$

$$\frac{\partial B_z}{\partial t}+u_{\mathrm{dz}}\frac{\partial B_z}{\partial z}-B_z\frac{\partial u_{uz}}{\partial z}-s_m\frac{\partial^2 B_z}{\partial z^2}=0, \tag{17}$$

$$\frac{\partial^2\varphi_g}{\partial x^2}+\frac{\partial^2\varphi_g}{\partial y^2}+\frac{\partial^2\varphi_g}{\partial z^2}=\mu_g n_d. \tag{18}$$

Equations (10) and (18) are closed by the 3-D Poisson equation as

$$\frac{\partial^2\phi}{\partial x^2}+\frac{\partial^2\phi}{\partial y^2}+\frac{\partial^2\phi}{\partial z^2}-n_d+\delta_i n_i-\delta_e n_e=0. \tag{19}$$

We can normalize the physical quantities in the dusty plasma model, which are the number densities relative to the number density of dust grains in the initial state $(n_{d0}Z_{d0})$, as follows: where $n_d=\overline{n}_d/(n_{\mathrm{d0}}Z_{\mathrm{d0}})$ refers to the normalized density of the number of dust grains in the perturbed state, $n_e=\overline{n}_e/(n_{\mathrm{d0}}Z_{\mathrm{d0}})$ refers to the normalized density of the number density is the normalized number density of hot electrons in the perturbed state, $n_i=\overline{n}_i/(n_{\mathrm{d0}}Z_{\mathrm{d0}})$ is the normalized perturbed number density of ions, and u_d is the velocity of the negative dusty grains, which is normalized by the dust-acoustic speed $C_d=(\lambda_D\omega_{pd})$. The electrostatic potential force ϕ and φ_g the gravitational potential force are normalized by $(K_B T_{\mathrm{eff}})/e$. The space coordinates are normalized by the Debye length $(\lambda_D=(K_B T_{\mathrm{eff}}/(4\pi e^2 Z_{\mathrm{d0}}n_{\mathrm{d0}}))^{1/2})$, and the time (t) is normalized by the inverse of dusty plasma frequency $\omega_{pd}^{-1}=(m_d/4\pi n_{\mathrm{d0}}$

$Z_{d0}^2 e^2)^{1/2}$ while the quantities without units of measure that appear in the dusty plasma model after normalization are $\sigma_i = T_i/T_{\rm eff}$, $\sigma_{ir} = \sigma_i^4 \alpha_r/3$, $\sigma_e = T_e/T_{eff}$, $\sigma_{er} = \sigma_e^4 \alpha_r/3$, $\delta_i = n_{d0} Z_{d0}/n_{i0}$, $\delta_e = n_{e0}/n_{d0} Z_{d0}$. $\beta_1 = (\Psi)/(m_d n_{d0} d_w^2 \omega_{pd})$, β_1 is the damping coefficient in the dusty plasma system, where the shear viscosity is a physical property that depends on how the plasma responds to shear stress or the damping process occurs in the plasma. $\beta_2 = (4\eta_0/3)/(m_d n_{d0} d_w^2 \omega_{pd})$ is also the another coefficient of damping in the dusty plasma system, where bulk viscosity is a material property that determines how a plasma responds to compression [15–19] where $d_w < \lambda_D$ is the dust grains radius.

In order to investigate studying propagation in three-dimensional envelope dust-acoustic waves, we employ the standard reductive perturbation technique [23] to reduce the basic set of the fluid equations (10)–(19) to one an evolution equation. Consider strongly magnetized plasma and the wave propagates in the z direction with weak transverse perturbations.

We can stretch the independent variables in the dusty plasma model using the following stretched [23]:

$$\xi = \varepsilon\left(z - V_g t\right), \zeta = \varepsilon x, \eta = \varepsilon y \text{ and } \tau = \varepsilon^2 t, \tag{20}$$

where ε is the power of arranging the perturbed and greater than zero, and V_g is the group velocity of the proliferating dust-acoustic wave. The dependent variables in the dusty plasma model are expanded as follows:

$$n_s = 1 + \sum_{m=1}^{\infty} \varepsilon^m \sum_{L=-m}^{m} n_{sL}^{(m)}(\xi,\tau) \exp\left(iL(kz - \omega t)\right), n_s\,(s = d, i, e), \tag{21}$$

$$u_{dz} = u_{d0} + \sum_{m=1}^{\infty} \varepsilon^m \sum_{L=-m}^{m} \left(u_{dz\,L}^{(m)}(\xi,\tau)\right) \exp\left(iL(kz - \omega t)\right), \tag{22}$$

$$\left[u_{dx}, u_{dy}\right] = \sum_{m=1}^{\infty} \varepsilon^{m+1} \sum_{L=-m}^{m} \left[\left(u_{dx\,L}^{(m)}(\xi,\tau), u_{dy\,L}^{(m)}(\xi,\tau)\right) \exp\left(iL(kz - \omega t)\right)\right], \tag{23}$$

$$\varphi_g = \varphi_{g0} + \sum_{m=1}^{\infty} \varepsilon^m \sum_{L=-m}^{m} \varphi_{gL}^{(m)}(\xi,\tau) \exp\left(iL(kz - \omega t)\right), \tag{24}$$

$$\varphi = \sum_{m=1}^{\infty} \varepsilon^m \sum_{L=-m}^{m} \varphi_L^{(m)}(\xi,\tau) \exp\left(iL(kz - \omega t)\right), \tag{25}$$

$$B_z = B_0 + \sum_{m=1}^{\infty} \varepsilon^m \sum_{L=-m}^{m} B_{zL}^{(m)}(\xi,\tau) \exp\left(iL(kz - \omega t)\right), \tag{26}$$

where ω is the angular frequency, and k is the real variable wave number. We take the remainder that all functions in the model satisfy the reality condition. By substituting equations (21)–(26) into the basic set of equations (10)–(20), the first order in ε gives, namely, the first harmonic mode of the carrier wave (i.e., $m = 1$ and $L = 1$). we get the following relations:

$$\begin{aligned} n_{d1}^{(1)} &= b_1 \phi_1^{(1)}, \\ u_{d1}^{(1)} &= b_2 \phi_1^{(1)}, \\ B_1^{(1)} &= b_3 \phi_1^{(1)}, \\ \varphi_{g1}^{(1)} &= b_4 \phi_1^{(1)}, \end{aligned} \tag{27}$$

where b_1, b_2, b_3, and b_4 are given in the appendix. From the perturbed first order of Poisson's equation, we obtain a linear equation, which is the linear dispersion relation in the dust plasma model under study.

$$\omega^2 - 2k u_{d0} \omega + h_3 = 0, \tag{28}$$

where

$$\begin{aligned} h_0 &= -k^2 - \delta_e \sigma_e - \delta_i \sigma_i, \\ h_1 &= k^2\left(15 r_1 + 8 r_2 - 9 u_{d0}^2\right), \\ h_2 &= 9k^2 (R_1 - 1), \\ h_3 &= \frac{h_0 h_1 + h_2 - 9 h_0 \mu_g \sigma_g}{9 h_0}, \\ r_1 &= \sigma_e \mu_e + \sigma_i \mu_i, \\ r_2 &= \sigma_{er} \mu_{er} + \sigma_{ir} \mu_{ir}. \end{aligned} \tag{29}$$

The linear dispersion relation in equation (28) has two roots for real values of k. The second-order $(m = 2)$, reduced the equations with harmonic modes $(L = 1)$, we get

$$n_{d1}^{(2)} = b_1\varphi_1^{(2)} + b_5\frac{\partial\phi_1^{(1)}}{\partial\xi},$$

$$u_{d1}^{(2)} = b_2\varphi_1^{(2)} + b_6\frac{\partial\varphi_1^{(1)}}{\partial\xi}, \tag{30}$$

$$B_1^{(2)} = b_3\varphi_1^{(2)} + b_7\frac{\partial\varphi_1^{(1)}}{\partial\xi},$$

$$\begin{aligned} \phi_{g1}^{(2)} &= b_4\varphi_1^{(2)} + h_8\frac{\partial\varphi_1^{(1)}}{\partial\xi}, \\ n_i &= -\sigma_i\varphi_1^{(2)}, \\ n_e &= \sigma_e\varphi_1^{(2)}, \end{aligned} \tag{31}$$

$$u_{\mathrm{d}x} = \frac{iB_0b_3s_1}{\omega}\frac{\partial\varphi}{\partial\eta} + \frac{-i\left(15b_1r_1 + 9R_1 + 8b_1r_2 + 9b_4\sigma_g - 9\right)}{9\omega}\frac{\partial\varphi}{\partial\zeta}, \tag{32}$$

$$u_{\mathrm{d}y} = \frac{iB_0b_3s_1}{\omega}\frac{\partial\varphi}{\partial\zeta} + \frac{-i\left(15b_1r_1 + 9R_1 + 8b_1r_2 + 9b_4\sigma_g - 9\right)}{9\omega}\frac{\partial\varphi}{\partial\eta}, \tag{33}$$

where b_5, b_6, b_7, and b_8 are given in the appendix. An explicit compatibility (consistency) condition is fulfilled via the following relation:

$$\begin{aligned} V_g &= \frac{\partial\omega}{\partial k}, \\ V_g &= V_{gr} + V_{gi}. \end{aligned} \tag{34}$$

The compatibility condition in equation (34) is exemplified by the group velocity of the dust-acoustic waves without the vector sign, which is defined in terms of frequency. It is seen that the group velocity is composed of real (V_{gr}) and imaginary (V_{gi}) parts, where V_{gr} and V_{gi} be in the appendix where the second harmonic modes ($m = L = 2$) arising from the nonlinear self-interaction of the carrier dust-acoustic waves are obtained in terms of $(\varphi_1^{(1)})^2$ as

$$\begin{aligned} n_{d2}^{(2)} &= b_9\left(\varphi_1^{(1)}\right)^2, \\ u_{d2}^{(2)} &= b_{10}\left(\varphi_1^{(1)}\right)^2, \\ B_2^{(2)} &= b_{11}\left(\varphi_1^{(1)}\right)^2, \\ \phi_{g2}^{(2)} &= b_{12}\left(\varphi_1^{(1)}\right)^2, \end{aligned} \tag{35}$$

$$\begin{aligned} n_{e2}^{(2)} &= b_{13}\left(\varphi_1^{(1)}\right)^2, \\ n_{i2}^{(2)} &= b_{14}\left(\varphi_1^{(1)}\right)^2, \\ \varphi_2^{(2)} &= b_{15}\left(\varphi_1^{(1)}\right)^2, \end{aligned} \tag{36}$$

where $b_9, \ldots,$ and b_{15} are given in the appendix. The nonlinear self-interaction of the carrier dust-acoustic wave also leads to the creation of a zeroth-order harmonic where its strength is determined analytically by taking the $L = 0$ components of the second order and the reduced equations of the third order, which can be expressed as a function of $|\varphi_1^{(1)}|^2$ as

$$\begin{aligned} n_{d0}^{(2)} &= b_{17}\left|\varphi_1^{(1)}\right|^2, \\ u_{d0}^{(2)} &= b_{18}\left|\varphi_1^{(1)}\right|^2, \\ B_z^{(2)} &= b_{19}\left|\varphi_1^{(1)}\right|^2, \\ n_{i0}^{(2)} &= b_{20}\left|\varphi_1^{(1)}\right|^2, \end{aligned} \tag{37}$$

$$\begin{aligned} n_{e0}^{(2)} &= b_{21}\left|\varphi_1^{(1)}\right|^2, \\ \phi_{g0}^{(2)} &= b_{16}, \\ \varphi_0^{(2)} &= b_{22}\left|\varphi_1^{(1)}\right|^2, \end{aligned} \tag{38}$$

where $b_{16}, \ldots,$ and b_{22} are given in the appendix. Finally, the third-harmonic modes ($m = 3$ and $L = 1$), with the aid of equations (27)–(38), give a set of equations. The compatibility condition for these equations yields the type of the 3D-CGL equation

$$i\frac{\partial\varphi}{\partial\tau} + P_1\frac{\partial^2\varphi}{\partial\xi^2} + P_2\left(\frac{\partial^2\varphi}{\partial\zeta^2} + \frac{\partial^2\varphi}{\partial\eta^2}\right) + P_3\varphi|\varphi|^2 + iP_4\varphi = 0, \tag{39}$$

where P_1 is the dispersion coefficient, P_3 is the nonlinear coefficient, P_4 is the dissipative coefficient, and the coefficient P_2 is given in the appendix and $\varphi \equiv \varphi_1^{(1)}$, for simplicity.

4. Analytical Solutions of the Dissipative Dust-Acoustic Waves

In this part, we will apply the modified extended simple equation technique to get dust-acoustic wave solutions. Since equation (38) is complex, this equation can be converted into exactly the same form as follows [33, 35, 36]:

$$i\frac{\partial\varphi}{\partial\tau}+(R_0+iR_{01})\frac{\partial^2\varphi}{\partial\xi^2}+(R_2+iR_{22})\left(\frac{\partial^2\varphi}{\partial\zeta^2}+\frac{\partial^2\varphi}{\partial\eta^2}\right)+(R_3+iR_{33})\varphi|\varphi|^2+iP_4\varphi=0, \tag{40}$$

where $P_1=R_0+iR_{11}$, $P_2=R_2+iR_{22}$, and $P_3=(R_3+iR_{33})$. Assume the solution in a travelling waveform as follows:

$$\varphi(\xi,\eta,\zeta,\tau)=\rho(Y)\exp(-i\Omega(Y+\tau)), \tag{41}$$

where $Y=L_1\xi+L_2\eta+L_3\zeta$, where L_1, L_2, and L_3 are the direction cosine in the coordinates ξ,η and ζ and satisfy the relation $L_1^2=1-L_2^2+L_3^2$, and Ω is the constant determined later. By inserting equation (41) into equation (40) and separating real and imaginary terms, we obtain

$$d_1\frac{d^2\rho}{dY}+2d_2\frac{d\rho}{dY}+R_3\rho^3-d_3\rho=0, \tag{42}$$

$$d_4\frac{d^2\rho}{dY^2}-2d_5\frac{d\rho}{dY}+R_{33}\rho^3+d_6\rho=0, \tag{43}$$

where $d_1=L_1^2R_0+R_2(L_2^2+L_3^2)$, $d_2=L_1R_{11}+(L_2+L_3)R_{22}$, $d_3=(R_0+2R_2)\Omega^2$, $d_4=L_1^2R_{11}+R_{22}(L_2^2+L_3^2)$, $d_5=L_1R_0+(L_2+L_3)R_2$, and $d_6=P_4-\Omega(1+\Omega R_{11}+2\Omega R_{22})$. By combining the equal degree in equation (42) and equation (43) in one equation,

$$g_2\frac{d^2\rho}{dY^2}+-2g_3\frac{d\rho}{dY}+(R_3+R_{33})\rho^3+g_1\rho=0, \tag{44}$$

where $g_1=d_6-d_3$, $g_2=d_1+d_4$, and $g_3=d_2-d_5$.

Apply the homogeneous balance principle between the nonlinear term and a dispersion term of equation (44) and assume the solution as [36]

$$\rho(Y)=c_0+c_1\left(\frac{\partial G(Y)}{G(Y)}\right)+c_2\frac{1}{G(Y)}, \tag{45}$$

where c_0, c_1, and c_2 are the constants determined later, and $G(Y)$ satisfies the following Riccati equation:

$$\frac{\mathrm{d}^2G(Y)}{\mathrm{d}Y^2}+c_3\frac{\mathrm{d}G(Y)}{\mathrm{d}Y}+c_4=0, \tag{46}$$

where c_3 and c_4 are the arbitrary constants. By inserting equation (45) into equation (44) and collecting a power of $G(Y)$, we get a system of algebraic equations, and solving this system, we get the given constants given the physical parameters such as

$$c_0=\frac{-g_1^{1/2}}{(-R_3-R_{33})^{1/2}},\quad c_1=\frac{-(2g_2)^{1/2}}{(-R_3-R_{33})^{1/2}},\quad c_2=\frac{(2)^{1/2}g_1}{3g_2^{1/2}(-R_3-R_{33})^{1/2}}, \tag{47}$$

$$c_0=\frac{-g_1^{1/2}}{(-R_3-R_{33})^{1/2}},\quad c_1=\frac{(2g_2)^{1/2}}{(-R_3-R_{33})^{1/2}},\quad c_2=\frac{-(2)^{1/2}g_1}{3g_2^{1/2}(-R_3-R_{33})^{1/2}}, \tag{48}$$

$$c_0=\frac{g_1^{1/2}}{(-R_3-R_{33})^{1/2}},\quad c_1=\frac{-(2g_2)^{1/2}}{(-R_3-R_{33})^{1/2}},\quad c_2=\frac{(2)^{1/2}g_1}{3g_2^{1/2}(-R_3-R_{33})^{1/2}}, \tag{49}$$

$$c_0=\frac{g_1^{1/2}}{(-R_3-R_{33})^{1/2}},\quad c_1=\frac{(2g_2)^{1/2}}{(-R_3-R_{33})^{1/2}},\quad c_2=\frac{-(2)^{1/2}g_1}{3g_2^{1/2}(-R_3-R_{33})^{1/2}}. \tag{50}$$

The Riccati equation has solutions in references [20, 34, 37, 38].

(1) The hyperbolic functions solution

$$G(Y)=\exp\left(\frac{-c_3}{2}Y\right)\left(c_5\cosh\left[\acute{A}_1Y\right]+c_6\sinh\left[\acute{A}_1Y\right]\right), \tag{51}$$

with $c_6<c_5$, $(c_3^2-4c_4^2)^{1/2}>0$, and $\acute{A}_1=(c_3^2-4c_4^2)^{1/2}$.

(2) The trigonometric functions solution

$$G(Y)=\exp\left(\frac{-c_3}{2}Y\right)\left(c_7\cos\left[\acute{A}_2Y\right]+c_8\sin\left[\acute{A}_2Y\right]\right), \tag{52}$$

with $c_7>c_8$, $(c_3^2-4c_4^2)^{1/2}<0$, and $\acute{A}_2=(c_3^2-4c_4^2)^{1/2}/i$,

(3) The exponential function

$$G(Y)=\exp\left(\frac{-c_3}{2}Y\right)(c_9+c_{10}),\text{with}\left(c_3^2-4c_4^2\right)^{1/2}=0, \tag{53}$$

where $c_3, c_4, \ldots,$ and c_{10} are the arbitrary constants, satisfying the above conditions

5. Numerical Results and Discussion

In this section, first, we conduct an analytical study on the behavior of the wave solution in equation (51) using one of the constants (47)–(50) and how it is affected by the physical quantities present in the dusty plasma system.

In our present investigation, we consider the role that physical quantities present in a dusty plasma system play in the mode in which the type of solution wave appears. As the direction of wave propagation L_3 changes, that is, when the direction of wave propagation decreases, this leads to the emergence of another type of wave behavior, which is the shock-like wave whereas, when the direction of wave propagation is large, the solitary wave appears, that is, when the physical values in the system are fixed and the value of the direction of wave propagation decreases. It also happens that when the unperturbed number density of electrons increases, it in turn leads to an increase in the unperturbed number density of ions through the state of neutralization, and thus, the shock-like wave appears. While the opposite is that when the unperturbed number density of electrons n_{e0} decreases, it in turn leads to the emergence of the soliton wave.

5.1. Soliton Structures. In this subsection, we are interested to investigate the impact of different compositional parameters on the dust-acoustic solitary waves (DASW) propagated in the considered dusty plasma medium by using the solution (51). To do so, we have analysed the negative solitary potential versus the space coordinate Y for the variation of different physical parameters, and it is discussed below in brief: the constraint of the soliton structures, when L_3 is large where this is the direction of propagation of the wave, and this leads to L_1 and L_2 being smaller.

Figure 1(a) shows the effect of the energy of the electrons on the amplitude and energy width of the dust soliton acoustic wave. We find that when the energy of the electron increases, this leads to an increase in the potential energy of the dusty soliton acoustic waves and also a slight expansion in the width of the soliton wave. Figure 1(b) shows that when the ion energy increases, it significantly affects the amplitude and energy width of the dust-acoustic soliton wave. We find that when the energy of the ions increases, this leads to an increase in the potential energy of the dust-acoustic soliton waves and also an expansion in the width of the soliton wave greater than in the case of increasing the energy of the electrons. Figure 1(c) shows that when the electron energy, i.e., the temperature ratio σ_e of the relative electrons increases, it significantly affects the amplitude and energy width of the dust-acoustic soliton wave. We find that when this energy increases, this leads to a decrease in the potential energy of the dusty soliton sound waves and also contract in the width of the soliton wave. Figure 1(d) shows that when the wave number k decreases, it greatly affects the amplitude and power width of the acoustic dust wave. We find that this potential energy increases significantly and also leads to an expansion in the width of the dusty soliton wave. In other words, when the wave number k increases, this leads to a decrease in the wavelength and thus increases the radiated energy, i.e., as the wavelength involved increases, the radiated energy tends to be, the (EMR) values are lower, and the frequency is also lower.

5.2. Shock-like Structures (Kink Wave). When inserting the solution (52) in the travelling wave (41), obtaining the kink wave and taking into account the values of the constants ((47), (47), or (49)). The constraint of the kink wave structures, when L_3 is smaller where this is the direction of propagation of the wave in a very narrow trajectory, leads to L_1 and L_2 being larger or when the unperturbed number density of electrons is greater than from the first case, i.e., $n_{e0} = 0.12\,\mathrm{cm}^{-3}$. This trajectory is clear that the higher temperature ratio σ_e of the electrons increases the wave energy of kink wave and its width as shown in Figure 2(a). Figure 2(b) shows the path of the energy of the zigzag wave and its width. It is clear that the higher temperature ratio of the ions increases the energy of the dust wave, and its width is also greater than it is in the case of increasing the energy of the electrons as shown in Figure 2(a). This indicates that when the thermal energy of the ions increases, this leads to an increase in the energy wave. Figure 2(c) shows the path of the dust wave energy and width, and it is clear that the higher temperature ratio of the radiating electrons σ_{er} reduces the energy of the dust wave, and its width is also clearly larger. Figure 2(d) shows the path of the kink wave energy and width, and it is clear that increasing the wavenumber k leads to an increase in the energy of the dust wave, and its width is also clearly larger.

5.3. Periodic Wave Structures. Introducing the solution (53) into the travelling wave (41), we obtain another type of waveform solution, which gives us a type of periodic wave, given the values of the constants ((47), (47), or (49)). These waves can be considered the electromagnetic waves, and these vector fields have a sine waveform, are oriented at right angles to each other, and oscillate perpendicular to the direction of dust-acoustic wave travel (Figure 3). It is clear that when the temperature ratio σ_e increases in the dusty plasma system, the nonlinearity in the system decreases, and this leads to a decrease in the energy of the electromagnetic wave and a decrease in the width of that wave as shown in Figure 3(a). Figure 3(b) shows that when the wave number k increases, that is, when the wavelength decreases, the energy of the electromagnetic wave decreases because the frequency decreases.

The dust-acoustic periodic travelling wave, when the value cosine in the direction of the wave propagation is large, appears, i.e., $L_3 = 0.72$. Figure 4(a) shows the periodic sharp wave type, and the effect of the electron temperature ratio on the behavior of the periodic wave. where the electromagnetic potential energy increases, when the electron temperature ratio increases. While Figure 4(b) shows the effect of the electron radiation temperature ratio on the behavior of the

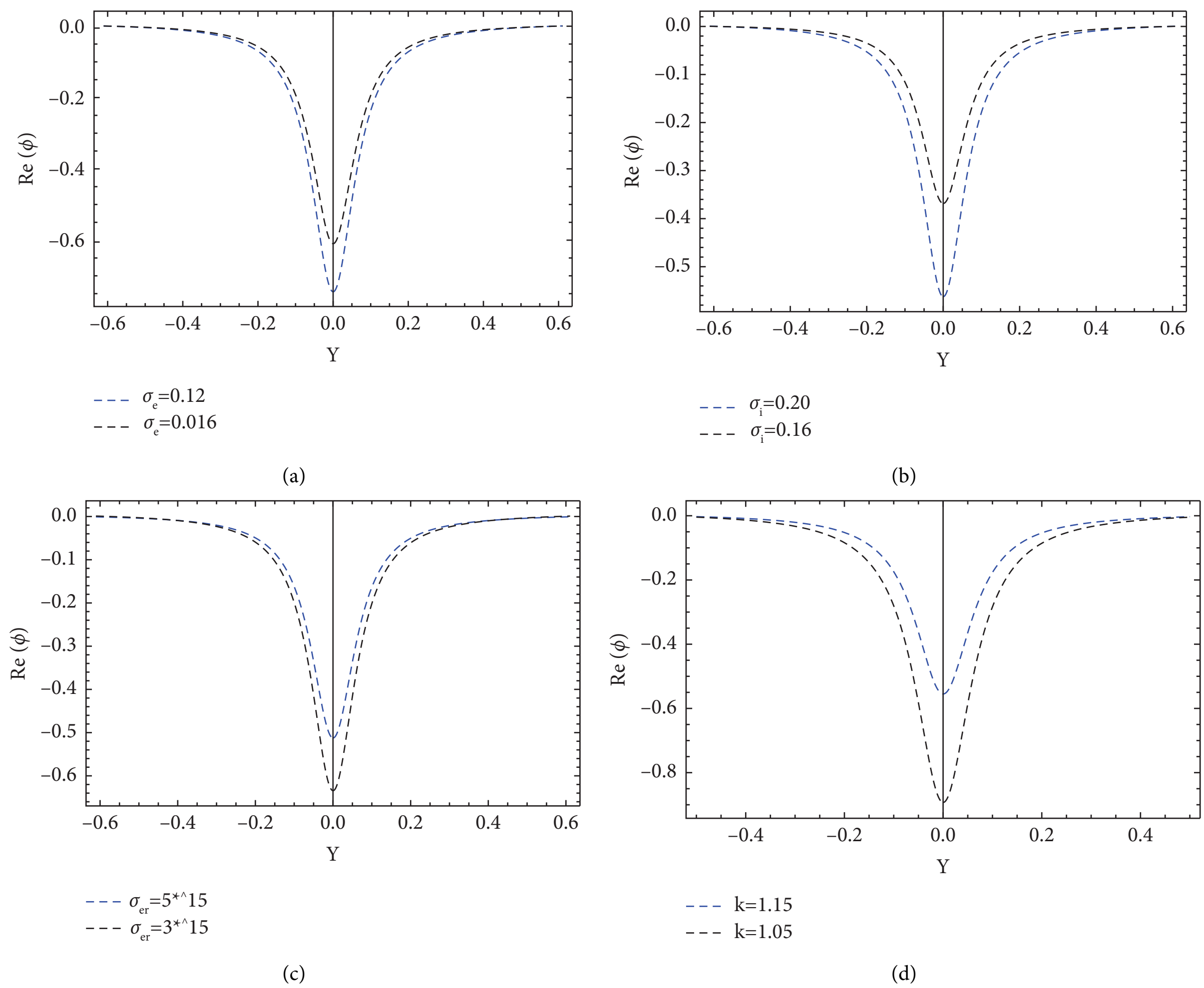

FIGURE 1: (Color online) (a): Two-dimensional profile of the solitary pulse for different values of σ_e. (b): Two-dimensional profile of the solitary pulse for different values of σ_i. (c): Two-dimensional profile of the solitary pulse for different values of σ_{er}. (d): Two-dimensional profile of the solitary pulse for different values of k, for $n_{e0} = 0.02\,\text{cm}^{-3}$, $n_{d0} = 12 \times 10^{-6}\,\text{cm}^{-3}$, $Z_{d0} = 500$, $n_{i0} = n_{e0} + Z_{d0}n_{d0}$, $T_e = 2.5 \times 10^4$ K, $T_i = 2 \times 10^3$ K, $R_1 = 0.018$, $u_{d0} = 0.015$, $\mu_g = 0.01$, $s_1 = 0.35$, $a_1 = 0.13$, $\beta_1 = 0.013$, $\beta_2 = 0.015$, $L_2 = 0.7, L_1 = 0.7$, $s_m = 0.003$, $\Omega = 0.03$, $B_0 = 0.025$, $c_3 = 0.8$, $c_4 = 0.2$, $c_5 = 1.6$, $c_6 = (-0.001)^{1/2}$.

periodic sharp wave, we find that when the electron radiation temperature ratio increases, it leads to a decrease in the wave amplitude.

6. Summarize

We investigated the properties of physical parameters on a dust-acoustic wave propagation of electrostatic dust in magnetized plasma containing isothermal electrons and hot ions in the presence of a magnetic field. Standard reductionist perturbation theory is used to derive the corresponding 3D-CGL equation that governs the dynamics. One of the useful results is the link between the emergence of soliton waves and electromagnetic waves, as well as between shock-like waves and periodic carrier waves. This means that when the wave propagation direction is large, which is also the direction of the magnetic field, the soliton wave appears whereas when the wave propagation direction is small, that is, the farther it is from the perpendicular direction of the magnetic field, the shock-like wave appears.

The advantage of using the method under study over the standard method is that when we used the harsh method, we get two waveforms using the same solution [39, 40], but here we get three waveforms for the same solution.

The present work applies to understanding the propagation and formations of dust waves in the attractive particle dust cloud when radiation pressure and strong coupling effects are simultaneously present in the dusty plasma system. The results can also be useful in understanding the nonlinear propagation of acoustic waves of dispersed dust in the viscomagnetic viscosity laboratory that has been used in the fundamental study of nonlinear dust activities in the dust cloud and astrophysical consequences.

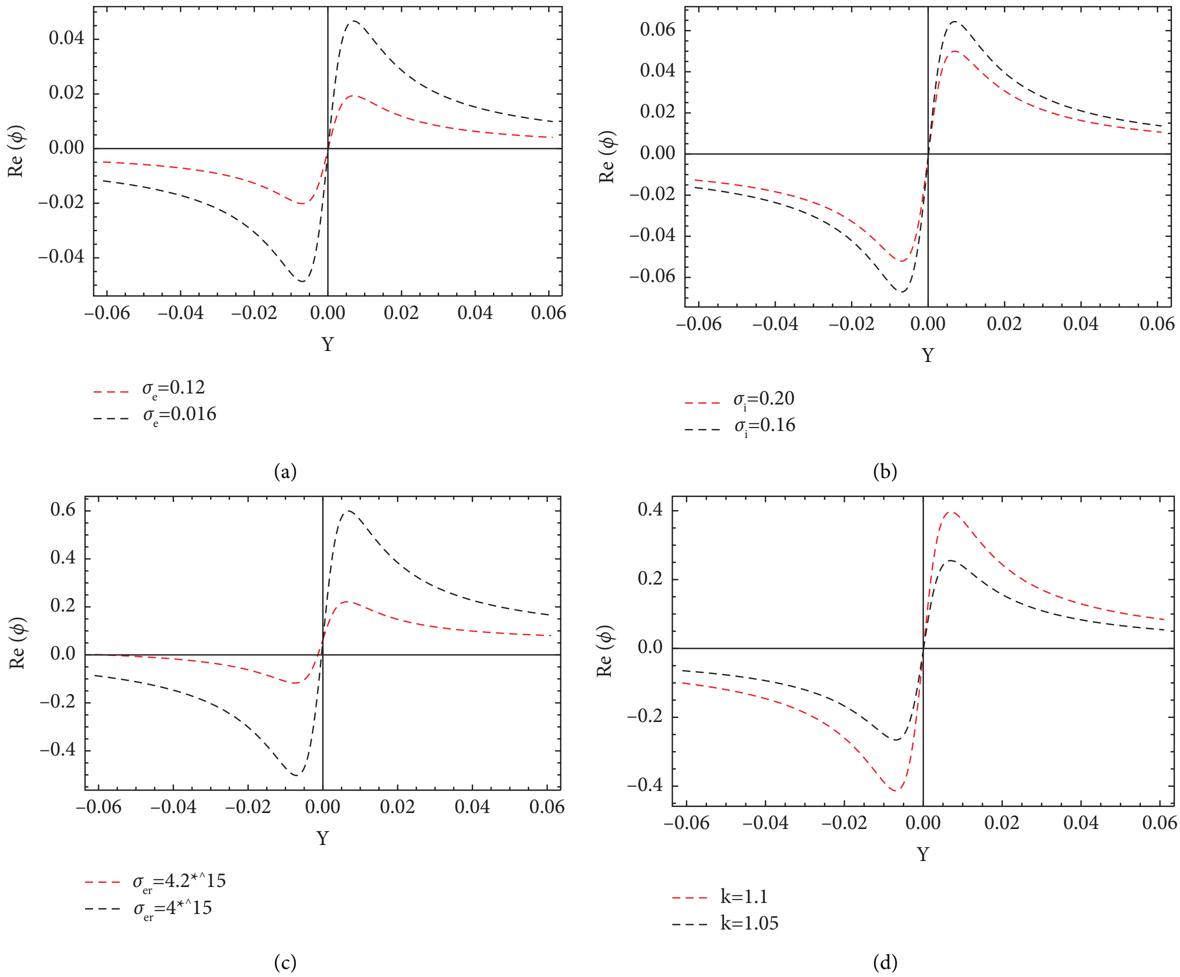

Figure 2: (Color online): (a): Two-dimensional profile of the shock-like pulse for different values of σ_e. (b): Two-dimensional profile of the shock-like pulse for different values of σ_i. (c): Two-dimensional profile of the shock-like pulse for different values of σ_{er}. (d): Two-dimensional profile of the shock-like pulse for different values of k, for $n_{e0} = 10\,\text{cm}^{-3}$, $n_{d0} = 10^{-4}\,\text{cm}^{-3}$, $Z_{d0} = 500$, $n_{i0} = n_{e0} + Z_{d0}n_{d0}$, $T_e = 2.4 \times 10^4$ K, $T_i = 2 \times 10^3$ K, $R_1 = 0.018$, $u_{d0} = 0.015$, $\mu_g = 0.0013$, $s_1 = 0.35$, $a_1 = 0.13$, $\beta_1 = 0.013$, $\beta_2 = 0.015$, $L_2 = 0.64$, $L_3 = 0.64$, $s_m = 0.003$, $\Omega = 0.03$, $B_0 = 0.025$, $c_3 = 0.8$, $c_4 = 0.2$, $c_5 = 1.6$, $c_6 = (-0.001)^{1/2}$.

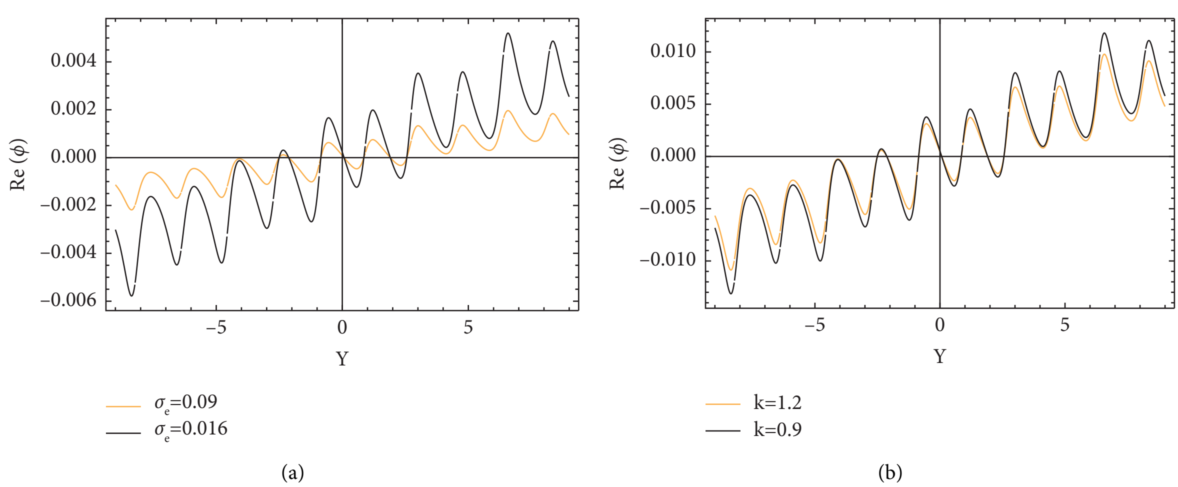

Figure 3: (Color online): (a): Two-dimensional profile of the electromagnetic pulse for different values of σ_e. (b): Two-dimensional profile of the electromagnetic pulse for different values of k. For $n_{e0} = 10\,\text{cm}^{-3}$, $n_{d0} = 10^{-4}\,\text{cm}^{-3}$, $Z_{d0} = 500$, $n_{i0} = n_{e0} + Z_{d0}n_{d0}$, $T_e = 2.4 \times 10^4$ K, $T_i = 2 \times 10^3$ K, $R_1 = 0.018$, $u_{d0} = 0.015$, $\mu_g = 0.0013$, $s_1 = 0.35$, $a_1 = 0.13$, $\beta_1 = 0.013$, $\beta_2 = 0.015$, $L_2 = 0.14$, $L_3 = 0.14$, $s_m = 0.003$, $\Omega = 0.03$, $B_0 = 0.025$, $c_3 = 0.8$, $c_4 = 0.2$, $c_5 = 1.6$, $c_6 = (-0.001)^{1/2}$.

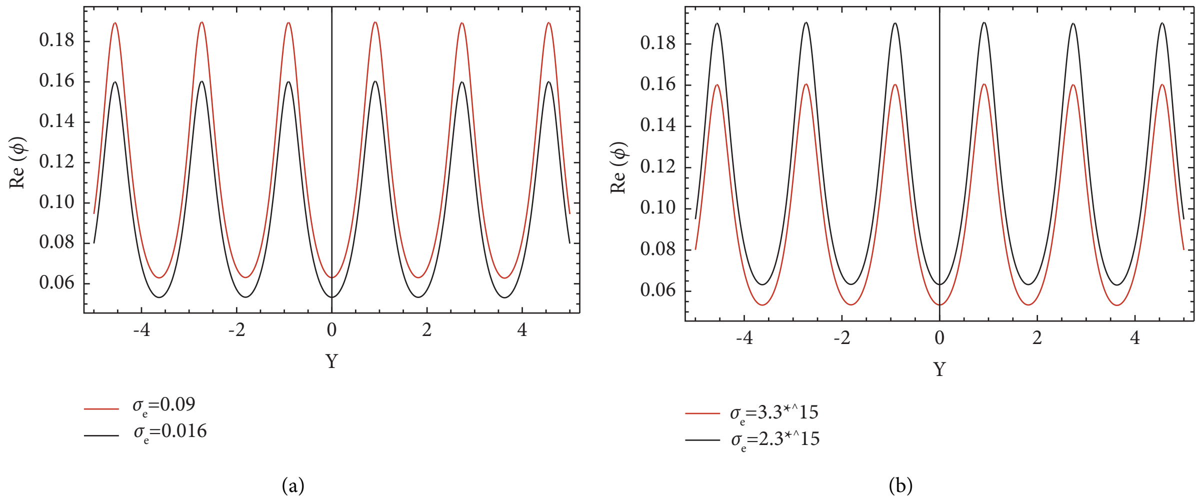

FIGURE 4: (Color online): (a): Two-dimensional profile of the periodical pulse for different values of σ_e. (b): Two-dimensional profile of the periodical pulse for different values of σ_{er}. For $n_{e0} = 10\,\text{cm}^{-3}$, $n_{d0} = 10^{-4}\,\text{cm}^{-3}$, $Z_{d0} = 500$, $n_{i0} = n_{e0} + Z_{d0}n_{d0}$, $T_e = 2.4 \times 10^3$ K, $T_i = 2 \times 10^3$ K, $R_1 = 0.018$, $u_{d0} = 0.015$, $\mu_g = 0.0013$, $s_1 = 0.35$, $a_1 = 0.13$, $\beta_1 = 0.013$, $\beta_2 = 0.015$, $L_2 = 0.64$, $L_3 = 0.64$, $s_m = 0.003$, $\Omega = 0.03$, $B_0 = 0.025$, $c_7 = 0.8$, $c_8 = 0.2$, $c_9 = 1.6$, $c_{10} = (-0.001)^{1/2}$.

Appendix

A: Constants

$$r_1 = \sigma_e\mu_e + \sigma_i\mu_i, r_2 = \sigma_{er}\mu_{er} + \sigma_{ir}\mu_{ir},$$

$$b_1 = \frac{9k^2(1-R_1)}{k^2\left(15r_1 + 8r_2 - 9u_{d0}^2\right) + 18ku_{d0}\omega - 9\left(\mu_g\sigma_g + \omega^2\right)},$$

$$b_2 = \frac{9k(1-R_1)(ku_{d0} - \omega)}{k^2\left(-15r_1 - 8r_2 + 9u_{d0}^2\right) - 18ku_{d0}\omega + 9\left(\mu_g\sigma_g + \omega^2\right)},$$

$$b_3 = \frac{9B_0k^2(-1+R_1)}{k^2\left(15r_1 + 8r_2 - 9u_{d0}^2\right) + 18ku_{d0}\omega - 9\left(\mu_g\sigma_g + \omega^2\right)},$$

$$b_4 = \frac{9k(1-R_1)\mu_g}{k^2\left(-15r_1 - 8r_2 + 9u_{d0}^2\right) - 18ku_{d0}\omega + 9\left(\mu_g\sigma_g + \omega^2\right)},$$

$$b_5 = \frac{162\,i\,k(1-R_1)\left(k^2u_{d0}V_g + \mu_g\sigma_g - k\left(u_{d0} + V_g\right)\omega + \omega^2\right)}{\left(k^2\left(15r_1 + 8r_2 - 9u_{d0}^2\right) + 18ku_{d0}\omega - 9\left(\mu_g\sigma_g + \omega^2\right)\right)^2},$$

$$b_6 = \frac{b_{61} + b_{62} + b_{63}}{b_4},$$

$$b_7 = \frac{b_{71} + b_{72} + b_{73}}{(ku_{d0} - \omega)b_5},$$

$$b_8 = \frac{b_{81}}{b_5},$$

$$
\begin{aligned}
b_9 &= \frac{b_{91}}{b_{92}},\\
b_{61} &= 9ik\left(R_1-1\right)\left(15k^2 r_1 V_g + 8k^2 r_2 V_g + 9k^2 u_{d0}^2 V_g + 18u_{d0}\mu_g\sigma_g - 9V_g\mu_g\sigma_g\right),\\
b_{62} &= -9ik\left(R_1-1\right)\left(15k^2 r_1 + 8k^2 r_2 + 9k^2 u_{d0}^2 + 18k^2 u_{d0} V_g + 9\mu_g\sigma_g\right),\\
b_{63} &= 81ik\omega^2\left(R_1-1\right)\left(V_g + 2u_{d0}\right) - 81i\omega^3\left(R_1-1\right),\\
b_{71} &= 18B_0k^2\left(R_1-1\right)\left(15k^3 r_1 s_m + 8k^3 r_2 s_m - 9k^3 s_m u_{d0} + 9ik^2 u_{d0} V_g - 9ks_m\mu_g\sigma_g + 9iu_{d0}\mu_g\sigma_g\right),\\
b_{72} &= 162B_0k\left(R_1-1\right)\left(2k^3 u_{d0} s_m - ik^2 u_{d0}^2 - 2ik^2 u_{d0} V_g - i\mu_g\sigma_g\right)\omega,\\
b_{73} &= -162B_0k^2\left(R_1-1\right)\left(ks_m - 2iu_{d0} - iV_g\right)\omega^2 - 162iB_0k\omega^3,\\
b_{81} &= 18i\left(R_1-1\right)\mu_g\left(k\left(15r_1 + 8r_2 + 9u_{d0}\left(Vg - u_{d0}\right)\right) + 9\omega\left(Vg - u_{d0}\right)\right),\\
b_{91} &= 2k - 27b_2^2k\left(4k^2 + \delta_e\sigma_e + \sigma_i\delta_i\right) + kb_1^2\left(15r_1 - 16r_2\right)\left(4k^2 + \delta_e\sigma_e + \sigma_i\delta_i\right)\\
&\quad + 27(R_1-1)\left(\delta_e\sigma_e^2 - \delta_i\sigma_i^2\right) + 54b_1b_2\left(4k^2 + \delta_e\sigma_e + \sigma_i\delta_i\right)\left(ku_{d0} - \omega\right),\\
b_{92} &= 3\left(16k^4\left(15r_1 + 8r_2 - 9u_{d0}^2\right)\right) + 288k^3 u_{d0}\omega + 72ku_{d0}\left(\delta_e\sigma_e + \sigma_i\delta_i\right)\omega - 9\left(\delta_e\sigma_e + \sigma_i\delta_i\right)\\
&\quad \cdot\left(\mu_g\sigma_g + 4\omega^2\right) + 4k^2\left(-9R_1 + \left(15r_1 + 8r_2 - 9u_{d0}\right)\left(\delta_e\sigma_e + \sigma_i\delta_i\right) - 9\left(\mu_g\sigma_g + 4\omega^2 - 1\right)\right),\\
b_{10} &= \frac{-b_{101} - b_{102}}{b_{92}},\\
b_{11} &= \frac{b_{111} + b_{112}}{b_{113}},\\
b_{12} &= \frac{b_{121}}{b_{122}},\\
b_{13} &= \frac{b_{131} + b_{132}}{b_{122}},\\
b_{101} &= 3b_1b_2 16k^4\left(15r_1 + 8r_2\right) - 9\mu_g\sigma_g\left(\delta_e\sigma_e + \sigma_i\delta_i\right) + 4k^2 9 - 9R_1 - 9\mu_g\sigma_g\\
&\quad + \left(15r_1 + 8r_2\right)\left(\delta_e\sigma_e + \sigma_i\delta_i\right),\\
b_{102} &= 2b_1^2\left(15r_1 - 16r_2\right)\left(4k^2 + \delta_e\sigma_e + \sigma_i\delta_i\right)\left(ku_{d0} - \omega\right) - 54k\left(ku_{d0} - \omega\right)\\
&\quad \cdot\left(b_2^2\left(4k^2 + \delta_e\sigma_e + \sigma_i\delta_i\right) - \left(R_1-1\right)\left(\delta_e\sigma_e^2 - \delta_i\sigma_i^2\right)\right),
\end{aligned}
\tag{A.1}
$$

$$
\begin{aligned}
b_{111} = {} & B_0 k\left(3b_1 b_2\left(16k^4\left(15r_1 + 8r_2\right)\right)\right) - 9\mu_g\sigma_g\left(\delta_e\sigma_e + \sigma_i\delta_i\right) + 4k^2 9 - 9R_1 - 9\mu_g\sigma_g \\
& + \left(15r_1 + 8r_2\right)\left(\delta_e\sigma_e + \sigma_i\delta_i\right) + 2b_1^2 k\left(15r_1 - 16r_2\right)\left(4k^2 + \delta_e\sigma_e + \sigma_i\delta_i\right)\left(ku_{d0} - \omega\right), \\
& b_{112} = 54k\left(ku_{d0} - \omega\right)\left(b_2^2\left(4k^2 + \delta_e\sigma_e + \sigma_i\delta_i\right)\right) - \left(R_1 - 1\right), \\
b_{113} = {} & 3\left(ku_{d0} - \omega\right) - 16k^4\left(15r_1 + 8r_2 - 9u_{d0}^2\right) - 288k^3 u_{d0}\omega - 72ku_{d0}\omega\left(\delta_e\sigma_e + \sigma_i\delta_i\right) \\
& + 9\left(\delta_e\sigma_e + \sigma_i\delta_i\right)\left(\mu_g\sigma_g + 4\omega^2\right) + 4k^2 9R_1 - \left(15r_1 + 8r_2 - 9u_{d0}^2\right)\left(\delta_e\sigma_e + \sigma_i\delta_i\right) \\
& + \left(-1 + \mu_g\sigma_g + 4\omega^2\right), \\
b_{121} = {} & \mu_g\begin{pmatrix} 27b_2^2 k\left(4k^2 + \delta_e\sigma_e + \sigma_i\delta_i\right) + k - b_1^2\left(15r_1 - 16r_2\right)\left(4k^2 + \delta_e\sigma_e + \sigma_i\delta_i\right) + \\ 27\left(R_1 - 1\right)\left(-\delta_e\sigma_e^2 + \delta_i\sigma_i^2\right) - 54b_1 b_2\left(4k^2 + \delta_e\sigma_e + \sigma_i\delta_i\right)\left(ku_{d0} - \omega\right) \end{pmatrix}, \\
b_{122} = {} & 6k\left(16k^4\left(15r_1 + 8r_2 - 9u_{d0}^2\right) + 288k^3 u_{d0}\omega + 72ku_{d0}\left(\delta_e\sigma_e + \sigma_i\delta_i\right)\omega - 9\left(\delta_e\sigma_e + \sigma_i\delta_i\right)\right. \\
& \left(\mu_g\sigma_g + 4\omega^2\right) + 4k^2\left(-9R_1 + \left(15r_1 + 8r_2 - 9u_{d0}^2\right)\left(\delta_e\sigma_e + \sigma_i\delta_i\right)\right) - 9\left(1 - \mu_g\sigma_g + 4\omega^2\right) \\
b_{131} = {} & \sigma_i\left(4b_1^2\left(15r_1 - 16r_2\right) - 108b_2 k^2 + 216b_1 b_2 k^2 u_{d0} + 3\delta_e\sigma_e^2\left(4k^4\left(15r_1 + 8r_2 - 9u_{d0}^2\right) - 9\mu_g\sigma_g\right)\right), \\
b_{131} = {} & 3\sigma_i^2 16k^4\left(15r_1 + 8r_2 - 9u_{d0}^2\right) - 9\delta_e\mu_g\sigma_e\sigma_g + 4k^2 9 - 9R_1\delta_e\left(15r_1 + 8r_2 - 9u_{d0}^2\right)\sigma_e \\
& + 108\sigma_i\omega\left(ku_{d0} - \omega\right)\left(4k^2 + \delta_e\sigma_e + \sigma_i\delta_i\right), \\
b_{14} = {} & \frac{b_{141} + b_{142}}{b_{122}}, \\
b_{15} = {} & \frac{b_{151}}{b_{122}}, \\
b_{17} = {} & \frac{-b_{171}}{b_{172}}, \\
b_{18} = {} & \frac{b_{181}}{b_{172}}, \\
b_{19} = {} & \frac{b_{191}}{\left(u_{d0} - V_g\right)b_{172}}, \\
b_{141} = {} & 4k^2\sigma_e\left(27b_2^2 - 15b_1^2 r_1 + 16b_2^2 r_2 - 54b_1 b_2 u_{d0} + 27\sigma_e + 108k^2 r_1\sigma_e - 27R_1\sigma_e - 108k^2 u_{d0}^2\sigma_e - 27\mu_g\sigma_e\sigma_g\right), \\
b_{142} = {} & 3\sigma_e 288k^3 u_{d0}\sigma_e\omega + 72k\left(b_1 b_2 + u_{d0}\delta_i\sigma_i\left(\sigma_i + \sigma_e\right)\right)\omega - 9\delta_i\sigma_i\left(\sigma_i + \sigma_e\right)\left(\mu_g\sigma_g + 4\omega^2\right) \\
& + 4k^2\left(\left(15r_1 + 8r_2 - 9u_{d0}^2\right)\delta_i\sigma_i\left(\sigma_i + \sigma_e\right) - 36\sigma_e\omega^2\right), \\
b_{151} = {} & 108k^2 b_2^2 + 4b_1^2 k^2\left(-15r_1 + 16r_2\right) + 216b_1 b_2 k\left(ku_{d0} - \omega\right) + 3\left(-\delta_e\sigma_e^2 + \delta_i\sigma_i^2\right) \\
& 4k^2\left(15r_1 + 8r_2 - 9u_{d0}^2\right) - 9\mu_g\sigma_g + 72ku_{d0}\omega - 36\omega^2, \\
b_{171} = {} & b_1^2\left(\left(-15r_1 + 16r_2\right) + 27b_2\left(b_2 + 2b_1\left(V_g - u_{d0}\right)\right)\right)\left(\delta_e\sigma_e + \sigma_i\delta_i\right)27 \\
& + \delta_e\sigma_e\left(\sigma_e - R_1\sigma_e + b_{16}\sigma_g\right) + \delta_i\sigma_i\left(b_{16}\sigma_g + \sigma_i\left(R_1 - 1\right)\right), \\
b_{172} = {} & 3\left(-9 + 9R_1 + \left(15r_1 + 8r_2 - 9\left(u_{d0} - V_g\right)^2\left(\delta_e\sigma_e + \sigma_i\delta_i\right)\right.\right., \\
b_{181} = {} & -b_1^2\left(-15r_1 + 16r_2\right)\left(V_g - u_{d0}\right)\left(\delta_e\sigma_e + \sigma_i\delta_i\right) + 27\left(u_{d0} - V_g\right)\delta_e\sigma_e\left(b_2^2 + \sigma_e - R_1\sigma_e b_{16}\sigma_g\right) \\
& + \delta_i\left(b_2^2 + b_{16}\sigma_g\right)\sigma_i + \delta_i\sigma_i^2\left(R_1 - 1\right) - 6b_1 b_2 - 9 + 9R_1 + \left(15r_1 + 8r_2\right)\left(\delta_e\sigma_e + \sigma_i\delta_i\right), \\
b_{191} = {} & B_0 b_1^2\left(15r_1 - 16r_2\right)\left(u_{d0} - V_g\right)\left(\delta_e\sigma_e + \sigma_i\delta_i\right) + 27\left(u_{d0} - V_g\right) - \delta_e\sigma_e\left(b_2^2 + \sigma_e - R_1\sigma_e + b_{16}\sigma_g\right) \\
& - \delta_i\left(b_2^2 + b_{16} + \left(R_1 - 1\right)\delta_i\sigma_i^2\right) + 6b_1 b_2\left(-9 + 9R_1 + \left(15r_1 + 8r_2\right)\left(\delta_e\sigma_e + \sigma_i\delta_i\right)\right),
\end{aligned}
$$

$$
\begin{aligned}
b_{20} &= \frac{b_{201}}{b_{172}}, \\
b_{21} &= \frac{b_{211}}{b_{172}}, \\
b_{22} &= \frac{b_{221}}{b_{172}}, \\
b_{201} &= \sigma_i 27 b_2^2 + b_1^2\left(-15r_1 + 16r_2\right) + 54 b_1 b_2\left(-u_{d0} + V_g\right) + 39 b_{16}\sigma_g + 9\sigma_i\left(R_1 - 1\right) \\
&\quad 15r_1 + 8r_2 - \left(u_{d0} - V_g\right)^2 \delta_e \sigma_e\left(\sigma_e + \sigma_i\right) \\
b_{211} &= \sigma_e - 27 b_2^2 + b_1^2\left(15r_1 - 16r_2\right) + 54 b_1 b_2\left(u_{d0} - V_g\right) - 27\left(\sigma_e - R_1\sigma_e + b_{16}\sigma_g\right) \\
&\quad + 3\left(15r_1 + 8r_2 - 9\left(u_{d0} - V_g\right)^2\right)\delta_i\sigma_i\left(\sigma_e + \sigma_i\right), \\
b_{221} &= -27 b_2^2 + b_1^2\left(15r_1 - 16r_2\right) + 54 b_1 b_2\left(u_{d0} - V_g\right) - 27 b_{16}\sigma_g \\
&\quad - 3\left(15r_1 - 16r_2 - 9\right)\left(u_{d0} - V_g\right)^2\left(\delta_e\sigma_e^2 + \sigma_i^2\delta_i\right), \\
P_1 &= \frac{P_{11}}{P_{12}}, \\
P_2 &= \frac{P_{21}}{P_{22}}, \\
P_3 &= \frac{-P_{31}}{P_{32}}, \\
P_4 &= \frac{P_{41}}{P_{42}}, \\
P_{11} &= k^2\left(-i\left(-15r_1 - 8r_2 + 9\left(u_{d0}^2 + a_1 b_6 u_{d0} V_g + a_1 b_8 V_g \sigma_g\right)\right) + a_1\left(15r_1 + 8r_2 + 9u_{d0}^2\right)\omega\right) \\
&\quad - 9\left(i + a_1\omega\right)\left(\mu_g\sigma_g - b_4\sigma_g + i b_6\omega + \omega^2\right) + k - 9 b_8\sigma_g + V_g - 9 b_6 - a_1 - 9 + 15 b_1 r_1 \\
&\quad + 8 b_1 r_2 + 9R_1 + 9 b_2 u_{d0} - 9 b_2 V_g + 9 b_4\sigma_g + 9i\left(2u_{d0} + 2a_1 b_6 V_g + a_1 b_8\sigma_g + 18 a_1 u_{d0}\omega^2\right) \\
&\quad + b_5 - i a_1 k^2\left(15r_1 + 8r_2\right)V_g + k\left(15r_1 + 8r_2 + 9u_{d0}\left(V_g - u_{d0}\right)\right)\left(1 - i\omega a_1\right) \\
&\quad + 9\left(u_{d0} - V_g\right)\omega\left(1 - i\omega a_1\right), \\
P_{12} &= 9 i b_1\left(k u_{d0} - \omega\right) + 9 b_2 k\left(-i + a_1 k u_{d0} - 2a_1\omega\right) + a_1 k^2\left(-9 + 15 b_1 r_1 + 9R_1 + 8 r_1 r_2 + 9 b_4\sigma_g\right) \\
&\quad + 9 b_1 k u_{d0}\omega - 9 b_1\omega^2, \\
P_{21} &= \left(i + a_1\omega\right)\left(k^2\left(-15r_1 - 8r_2 9u_{d0}^2\right)\omega + \omega 9 b_1\left(15r_1 + 8r_2\right) + 9\left(-1 + R_1 + \mu_g\sigma_g + \omega^2\right)\right) \\
&\quad - k u_{d0}\left(b_1\left(15r_1 + 8r_2\right) + 9\left(-1 + R_1 + b_4\sigma_g + 2\omega^2\right)\right), \\
P_{22} &= \omega\left(-k\left(9 i b_1 u_{d0} + a_1 k\left(-9 + 15 b_1 r_1 + 9R_1 + 8 b_1 r_2 + 9 b_4\sigma_g\right)\right) - 9 b_1\left(-i + a_1 k u_{d0}\right)\omega \right. \\
&\quad \left. + 9 a_1 b_1\omega^2 + 9 b_2 k\left(i - a_1 k u_{d0} + 2a_1\omega\right)\right),
\end{aligned}
\tag{A.2}
$$

$$
\begin{aligned}
P_{31} &= (i + a_1\omega)\left(k^2(-15r_1 - 8r_2 + 9u_{d0})\right) - 18ku_{d0}\omega + 9\left(\mu_g\sigma_g + \omega^2\right)162b_{10}b_2k^2 + 4b_1^3k^2(15r_1 - 4r_2) \\
&\quad +6b_1b_9k^2(-15r_1 - 4r_2) + 6b_1b_9k^2(-15r_1 + 16r_2) - 9\left(\delta_e\sigma_e^2(2b_{15} + \sigma_e)\right) - 2b_{15}\delta_i\sigma_i^2 + \delta_i\sigma_i^3 \\
&\quad \left(k^2\left(15r_1 + 8r_2 - 9u_{d0}^2\right) + 18ku_{d0}\omega - 9\left(\mu_g\sigma_g + \omega^2\right)\right) + 6(27b_{18}k(kb_2 + b_1(\omega - ku_{d0}))) \\
&\quad +b_1k(b_{17}k(16r_2 - 15r_1) + 27b_{10}(\omega - ku_{d0}) - 3(9b_{17}b_2k(\omega - ku_{d0}) + 9b_2b_9k(\omega - ku_{d0}) + b_{22})) \\
&\quad \left(\delta_e\sigma_e^2 - \delta_i\sigma_i^2\right)k^2\left(15r_1 + 8r_2 - 9u_{d0}^2\right) + 18ku_{d0}\omega - 9\left(\mu_g\sigma_g + \omega^2\right), \\
P_{32} &= 18\left(k^2\left(15r_1 + 8r_2 - 9u_{d0}^2\right) + 18ku_{d0}\omega - 9\left(\mu_g\sigma_g + \omega^2\right)\right)9ib_1(-\omega + ku_{d0}) + 9b_2k(-i + a_1ku_{d0}) \\
&\quad -2a_1\omega + a_1\left(k^2\left(15b_1r_1 - 9 + 9R_1 + 8b_1r_2 + 9b_4r_2 + 9b_4\sigma_g\right) + 9b_1ku_{d0}\omega - 9b_1\omega^2\right), \\
P_{41} &= -9ib_2k^3(\beta_1 + \beta_2), \\
P_{42} &= 9ib_1(-\omega + ku_{d0}) + 9b_2k(a_1ku_{d0} - i - 2a_1\omega) + a_1\left(k^2\left(15b_1r_1 - 9 + 9R_1 + 8b_1r_2 + 9b_4\sigma_g\right)\right) \\
&\quad +9b_1ku_{d0}\omega - 9b_1\omega^2,
\end{aligned}
\tag{A.3}
$$

B: The solution of the Riccati equation is

$$\frac{d^2H}{dx^2} + \beta\frac{dH}{dx} + \alpha H = 0, \tag{B.1}$$

$H \equiv H(x)$, we suppose that

$$H = \exp(rx), \tag{B.2}$$

is the solution of equation (B.1) where

$$\frac{dH}{dx} = r\exp(rx), \text{and } \frac{d^2H}{dx^2} = r^2\exp(rx). \tag{B.3}$$

The characteristic equation is

$$r^2 + \beta r + \alpha = 0, \tag{B.4}$$

where

$$
\begin{aligned}
r_1 &= \lambda_1, \\
r_2 &= \lambda_2,
\end{aligned}
\tag{B.5}
$$

where

$$
\begin{aligned}
\lambda_1 &= \frac{1}{2}\left(-\beta - \sqrt{\beta^2 - 4\alpha}\right), \\
\lambda_2 &= \frac{1}{2}\left(-\beta + \sqrt{\beta^2 - 4\alpha}\right).
\end{aligned}
\tag{B.6}
$$

The general solution is

$$H = c_1\exp(-\lambda_1x) + c_2\exp(-\lambda_2x). \tag{B.7}$$

When $\beta^2 - 4\alpha = 0$, this tends to $r_1 = r_2 = -\beta/2$, and the general solution is

$$H = \exp\left(\frac{-\beta}{2}x\right)(c_1 + c_2). \tag{B.8}$$

When $\beta^2 - 4\alpha < 0$, this tends to $r_1 \neq r_2$, and we define $r_1 = \lambda + i\mu$, $r_2 = \lambda - i\mu$, $i = \sqrt{-1}$, and

$$
\begin{aligned}
\cos(x) &= \frac{1}{2}(\exp(ix) + \exp(-ix)), \\
\sin(x) &= \frac{1}{2i}(\exp(ix) - \exp(-ix)).
\end{aligned}
\tag{B.9}
$$

The two solutions of the differential equation are

$$
\begin{aligned}
H_1 &= \exp((\lambda + i\mu)x), \\
H_2 &= \exp((\lambda - i\mu)x).
\end{aligned}
\tag{B.10}
$$

The general solution is

$$
\begin{aligned}
H &= c_3H_1 + c_4H_2, \\
H &= \exp(\lambda x)(c_3\exp(i\mu x) + c_4\exp(-i\mu x)), \\
H &= \exp(\lambda x)(c_3(\cos(\mu x) + i\sin(\mu x)) \\
&\qquad + c_4(\cos(\mu x) - i\sin(\mu x))), \\
H &= \exp(\lambda x)(c_3(\cos(\mu x)) + c_4(\sin(\mu x))).
\end{aligned}
\tag{B.11}
$$

When $\beta^2 - 4\alpha > 0$, this tends to $r_1 \neq r_2$, and we define $r_1 = \lambda + \mu$, $r_2 = \lambda - \mu$, and the general solution is

$$H = c_5H_1 + c_6H_2, \tag{B.12}$$

where

$$
\begin{aligned}
H_1 &= \exp(\lambda_1 x),\\
H_2 &= \exp(\lambda_2 x),\\
\lambda_1 &= \frac{-\beta-\mu}{2},\\
\lambda_2 &= \frac{-\beta+\mu}{2},\\
H &= \exp\left(\frac{-\beta}{2}x\right)\left(c_5\exp\left(\frac{-\mu x}{2}\right)+c_6\exp\left(\frac{\mu x}{2}\right)\right),\\
H &= \exp\left(\frac{-\beta}{2}x\right)\begin{pmatrix} c_5\left(\sinh\left(\frac{\mu x}{2}\right)-\cosh\left(\frac{\mu x}{2}\right)\right)+\\ c_6\left(\sinh\left(\frac{\mu x}{2}\right)+\cosh\left(\frac{\mu x}{2}\right)\right)\end{pmatrix},\\
H &= \exp\left(\frac{-\beta}{2}x\right)\left((c_5+c_6)\sinh\left(\frac{\mu x}{2}\right)+(-c_5+c_6)\cosh\left(\frac{\mu x}{2}\right)\right),\\
H &= \exp\left(\frac{-\beta}{2}x\right)\left(c_7\sinh\left(\frac{\mu x}{2}\right)+c_8\cosh\left(\frac{\mu x}{2}\right)\right),
\end{aligned}
\tag{B.13}
$$

where $c_7 > c_8$.

Data Availability

Data sharing applies to this article in references [30–32] as the datasets were generated or analyzed during the current study.

Conflicts of Interest

The authors declare that they have no conflicts of interest.

Authors' Contributions

All authors contributed equally to complete this work.

Acknowledgments

The authors express their gratitude to Princess Nourah Bint Abdulrahman University Researchers Supporting Project number PNURSP2023R2, Princess Nourah Bint Abdulrahman University, Riyadh, Saudi Arabia.

References

[1] M. Salimullah and P. K. Shukla, "On the stability of self-gravitating magnetized dusty plasmas," *Physics of Plasmas*, vol. 6, no. 3, pp. 686–691, 1999.

[2] A. M. Mirza, M. A. Sarwar, and M. S. Qaisar, "Effect of self-gravitation on the energy loss of pair of projectiles in dusty plasma," *Physics of Plasmas*, vol. 13, no. 5, Article ID 052106, 2006.

[3] V. Jatenco-Pereira, A. C.-L. Chian, and N. Rubab, "Alfvén waves in space and astrophysical dusty plasmas," *Nonlinear Processes in Geophysics*, vol. 21, no. 2, pp. 405–416, 2014.

[4] P. K. Shukla and I. Sandberg, "Radiation-condensation instability in a self-gravitating dusty astrophysical plasma," *Physical Review*, vol. 67, no. 3, Article ID 036401, 2003.

[5] N. S. Saini, Y. Ghai, and R. Kohli, "Dust acoustic dromions in a magnetized dusty plasma with superthermal electrons and ions," *Journal of Geophysical Research: Space Physics*, vol. 121, no. 6, pp. 5944–5958, 2016.

[6] A. A. Mamun, "Obliquely propagating dust-acoustic solitary waves in a magnetized dusty plasma," *Il Nuovo Cimento-B D*, vol. 20, no. 9, pp. 1307–1312, 1998.

[7] A. A. Mamun, "Compressive and rarefactive dust-acoustic solitary structures in a magnetized two-ion- temperature dusty plasms," *Astrophysics and Space Science*, vol. 260, pp. 507–514, 1999.

[8] N. N. Rao, P. K. Shukla, and M. Y. Yu, "Dust-acoustic waves in dusty plasmas," *Planetary and Space Science*, vol. 38, no. 4, pp. 543–546, 1990.

[9] P. K. Shukla, "Low-frequency modes in dusty plasmas," *Physica Scripta*, vol. 45, no. 5, pp. 504–507, 1992.

[10] F. Verheest, P. K. Shukla, N. N. Rao, and P. Meuris, "Dust-acoustic waves in self-gravitating dusty plasmas with fluctuating dust charges," *Journal of Plasma Physics*, vol. 58, no. 1, pp. 163–170, 1997.

[11] D. A. Mendis and M. Rosenberg, "Cosmic dusty plasma," *Annual Review of Astronomy and Astrophysics*, vol. 32, no. 1, pp. 419–463, 1994.

[12] C. K. Goertz, "Dusty plasmas in the solar system," *Reviews of Geophysics*, vol. 27, no. 2, pp. 271–292, 1989.

[13] W. F. El-Taibany, S. K. El-Labany, A. S. El-Helbawy, and A. Atteya, "Dust-acoustic solitary and periodic waves in magnetized self-gravito-electrostatic opposite polarity dusty plasmas," *Eur. Phys. J. Plus.*, vol. 137, no. 2, p. 261, 2022.

[14] M. R. Jana, A. Sen, and P. K. Kaw, "Collective effects due to charge-fluctuation dynamics in a dusty plasma," *Physical Review*, vol. 48, no. 5, pp. 3930–3933, 1993.

[15] S. Raut, S. Roy, S. Saha, and A. N. Das, "Effect of kinematic viscosity on ion acoustic waves in superthermal plasma comprising cylindrical and spherical geometry," *International Journal of Algorithms, Computing and Mathematics*, vol. 8, no. 4, p. 196, 2022.

[16] S. Roy, R. R. Kairi, and S. Raut, "Cylindrical and spherical dust–ion-acoustic shock solitary waves by Korteweg–de Vries–Burgers equation," *Brazilian Journal of Physics*, vol. 51, no. 6, pp. 1651–1660, 2021.

[17] S. Roy, S. Raut, and R. R. Kairi, "Nonlinear analysis of the ion-acoustic solitary and shock wave solutions for non-extensive dusty plasma in the framework of modified Korteweg–de Vries–Burgers equation," *Pramana*, vol. 96, no. 2, p. 67, 2022.

[18] S. Roy, S. Saha, S. Raut, and A. N. Das, "Studies on the effect of kinematic viscosity on electron-acoustic cylindrical and spherical solitary waves in a plasma with trapped electrons," *Journal of Applied Mathematics and Computational Mechanics*, vol. 20, no. 2, pp. 65–76, 2021.

[19] S. Raut, S. Roy, S. Saha, and A. N. Das, "Studies on the dust–ion–acoustic solitary wave in planar and non-planar super-thermal plasmas with trapped electrons," *Plasma Physics Reports*, vol. 48, no. 6, pp. 627–637, 2022.

[20] S. M. Ahmed, E. R. Hassib, U. M. Abdelsalam, R. E. Tolba, and W. M. Moslem, "Proliferation of soliton, explosive, shocklike, and periodic ion-acoustic waves in Titan's ionosphere," *Physics of Plasmas*, vol. 27, no. 8, Article ID 082903, 2020.

[21] R. E. Tolba, N. A. El-Bedwehy, W. M. Moslem, S. K. El-Labany, and M. E. Yahia, "Nonlinear structures: cnoidal, soliton, and periodical waves in quantum semiconductor

plasma," *Physics of Plasmas*, vol. 23, no. 1, Article ID 012111, 2016.
[22] J. L. Shohet, B. R. Barmish, H. K. Ebraheem, and A. C. Scott, "The sine-Gordon equation in reversed-field pinch experiments," *Physics of Plasmas*, vol. 11, no. 8, pp. 3877–3887, 2004.
[23] R. E. Tolba, W. M. Moslem, N. A. El-Bedwehy, and S. K. El-Labany, "Evolution of rogue waves in dusty plasmas," *Physics of Plasmas*, vol. 22, Article ID 043707, 2015.
[24] S. Guo and L. Mei, "Modulation instability and dissipative rogue waves in ion-beam plasma: roles of ionization, recombination, and electron attachment," *Physics of Plasmas*, vol. 21, no. 11, Article ID 112303, 2014.
[25] L. Brusch, A. Torcini, and M. Bär, "Nonlinear analysis of the Eckhaus instability: modulated amplitude waves and phase chaos with nonzero average phase gradient," *Physica D: Nonlinear Phenomena*, vol. 174, no. 1-4, pp. 152–167, 2003.
[26] S. Banik, R. K. Shikha, A. A. Noman et al., "First and second-order dust-ion-acoustic rogue waves in non-thermal plasma," *The European physical Journal D*, vol. 75, no. 2, p. 43, 2021.
[27] M. C. Cross and P. C. Hohenberg, "Pattern formation outside of equilibrium," *Reviews of Modern Physics*, vol. 65, no. 3, pp. 851–1112, 1993.
[28] A. Wierschem, H. Linde, and M. G. Velarde, "Internal waves excited by the Marangoni effect," *Physical Review*, vol. 62, no. 5, pp. 6522–6530, 2000.
[29] R. Sabry, W. M. Moslem, and P. K. Shukla, "Amplitude modulation of hydromagnetic waves and associated rogue waves in magnetoplasmas," *Physical Review*, vol. 86, no. 3, Article ID 036408, 2012.
[30] R. E. Tolba, A. Abdikian, N. S. Alharthi, M. E. Yahia, and W. M. Moslem, "Dust-acoustic Rossby waves in magnetized plasma," *The European Physical Journal Plus*, vol. 138, p. 541, 2023.
[31] S. Chen, "Theory of dissipative solitons in complex Ginzburg-Landau systems," *Physical Review*, vol. 78, Article ID 025601, 2008.
[32] S. Bhakta, R. K. Chhajlani, and R. P. Prajapati, "Effects of radiation pressure and polarization force on Jeans instability in magnetized strongly coupled dusty plasma," *Physica Scripta*, vol. 94, no. 4, Article ID 045603, 2019.
[33] J. M. Soto-Crespo, N. Akhmediev, and A. Ankiewicz, "Pulsating, creeping, and erupting solitons in dissipative systems," *Physical Review Letters*, vol. 85, no. 14, pp. 2937–2940, 2000.
[34] N. L. Tsintsadze, R. Chaudhary, H. A. Shah, and G. Murtaza, "Stability of a charged interface between a magnetoradiative dusty plasma and vacuum," *Physics of Plasmas*, vol. 14, no. 7, Article ID 073703, 2007.
[35] J. M. Soto-Crespo and N. Akhmediev, "Soliton as strange attractor: nonlinear synchronization and chaos," *Physical Review Letters*, vol. 95, no. 2, Article ID 024101, 2005.
[36] A. Ghafoor, S. Firdous, T. Zubair, A. Iftikhar, S. Zainab, and S. T. Mohyud-Din, "(G'/G, $1/G$)-Expansion method for generalized ZK, Sharma–Tasso–Olver (STO) and modified ZK equationsG'/G,1/G-Expansion method for generalized ZK, Sharma–Tasso–Olver (STO) and modified ZK equations," *QScience Connect*, vol. 1, p. 24, 2013.
[37] T. A. Thompson, "Gravitational instability in radiation pressure-dominated backgrounds," *The Astrophysical Journal*, vol. 684, no. 1, pp. 212–225, 2008.
[38] N. S. Alharthi and R. E. Tolba, "Propagation of different kinds of non-linear ion-acoustic waves in Earth's magnetosphere," *Astrophysics and Space Science*, vol. 367, no. 11, p. 113, 2022.
[39] A. Elmandoh, A. A. Fayad, R. E. Tolba, and W. M. Moslem, "Soliton, blow up, and shock-like ion-acoustic waves in magnetized plasma at Venus' ionosphere," *Indian Journal of Physics*, vol. 97, no. 8, pp. 2537–2545, 2023.
[40] W. M. Moslem, A. S. El-Said, R. E. Tolba, and H. Bahlouli, "Modifications of single walled carbon nanotubes by ion-induced plasma," *Results in Physics*, vol. 37, Article ID 105438, 2022.